Results of a dark matter search with a germanium detector in the Canfranc tunnel

E. García, A. Morales, J. Morales, M. L. Sarsa, A. Ortiz de Solórzano, E. Cerezo,
R. Núñez-Lagos, J. Puimedón, C. Sáenz, A. Salinas, and J. A. Villar
Instituto de Física Nuclear y Altas Energías, Facultad de Ciencias, Universidad de Zaragoza, 50009 Zaragoza, Spain

J. I. Collar and F. T. Avignone
Department of Physics and Astronomy, University of South Carolina, Columbia, South Carolina 29208

R. L. Brodzinski, H. S. Miley, and J. H. Reeves
Pacific Northwest Laboratory, Richland, Washington 99352

The results of a search for particle dark matter with a germanium detector at the Canfranc tunnel are reported. Contour limits for cross sections, masses, and local halo densities of dark matter particles interacting with Ge nuclei through spin-independent interactions are presented for an exposure of 130.7 kg day. The results and prospects of a search for the timing modulation of the signal are also reported.

I. INTRODUCTION

A fundamental question for cosmology, astrophysics, and particle physics is to discover the nature of the dark matter (DM) which may constitute most of the mass of the Universe. The challenge of its direct detection has prompted a large number of experimental searches [1,2].

The current picture [3] of DM features a mixed model (MDM) with a variety of components [baryonic, hot (HDM), and cold (CDM) dark matter] to the missing mass of the Universe. In addition, some fraction (if not all) of the hypothetical galactic halo mass could be accounted for by baryonic dark matter in the form of massive compact halo objects (MACHO's), a possibility that is now being actively investigated [4]. Searches for non-baryonic dark matter are also in progress and various kinds of candidates have been excluded or constrained in first-generation experiments by using, for instance, a germanium detector to measure the nuclear recoil produced by the CDM elastic scattering off Ge nuclei.

Most of the exclusion plots of masses and cross sections obtained so far [5–10] for CDM particles were derived under the assumption of a unique component of the DM, and they should be taken with caution. In fact, a significant reduction of the density allocated to the CDM component would essentially wash out most of the constraints reported up to now.

The method customarily used to determine the possible presence of a CDM component in a spectrum (by comparing the theoretically predicted CDM signal with the number of counts recorded in a given energy region) has been useful to exclude or constrain the most obvious cases such as those reported in this work. The nonappearance of a dark matter effect has imposed severe constraints on various models and candidates. However, it is very unlikely that this method of directly comparing signal to noise could succeed in detecting a small component of the DM signal clearly emerging from the background.

It is clear that ultralow background detectors with an energy threshold as low as possible are needed, and that any effort in improving the level of sensitivity of the detectors could be rewarding. Thus, in order to disentangle the expected signal from the background at such low energies, one has to design procedures to remove the dominant sources of background from the spectra: microphonics and electronic noise. Other background sources, inherent to the particular experimental devices (natural or induced radioactivity) are reduced by using state-of-the-art low background technology, by keeping the cosmogenic induced activity at minimum, and by employing passive and active shielding in a clean environment at an underground laboratory. The accumulated Compton distribution of the γ radioactive contamination and the β continuum of other impurities, as well as various x-ray peaks appearing in the low energy region of interest, can be estimated by Monte Carlo modeling and/or monitoring the impurities, although one must always keep in mind that these procedures are only approximations. The prospects for a successful direct search of cold dark matter particles, if they exist, certainly rely on the improvement that could be achieved in the background, energy threshold, and sensitivity of the detectors, but a convincing proof of the detection of CDM would need to show distinctive signatures of CDM in the data, not reproduced by background. The diurnal [11] or annual [12,13] modulations predicted for the dark matter signals are two such distinctive effects. Otherwise we are limited to simply narrowing the survival window of the CDM particle candidates as we improve our detector's performances.

We present here the results of a search for particle dark matter with a small germanium detector, carried out by the Zaragoza/USC/PNL Collaboration at the Canfranc tunnel (Spanish Pyrenees), after an exposure of 130.7 kg day. Preliminary results of this experiment have been published elsewhere [8,9].

II. PHENOMENOLOGICAL FRAMEWORK

If weakly interacting massive particles (WIMP's) form the galactic halos, they may interact with the detector nuclei producing a measurable nuclear recoil. The size and rate of the expected signal depend on the specific halo and particle physics models, and so do the CDM particle constraints derived from experiments.

The rate of detection of WIMP's producing a recoil T in the detector is given by [12]

$$\frac{dN}{dt\,dT} = N_D \frac{\rho_h}{m} \int_{v_{\min}(T)}^{v_{\max}} \frac{d\sigma}{dT}(v,T) f\mathbf{v}v d^3v \ ,$$

where T is the recoil energy of the target nucleus, $f(\mathbf{v})$ is the velocity distribution of the halo's CMD in the reference frame of the Earth, N_D is the total number of target nuclei, ρ_h is the local galactic halo density, and $d\sigma/dT$ is the differential scattering cross section given below. The mass of the CDM particle is denoted by m. The measured deposited energy E and the nuclear recoil energy T are connected by a relative efficiency (or quenching) Q factor [2,5]. The quantity $v_{\min}(T)$ is the minimum relative velocity a particle must have in order to leave an energy T in the detector, and $\mathbf{v}_{\max}$ is the maximum velocity of WIMP's relative to the detector, i.e., the vectorial sum of the galactic escape velocity $\mathbf{v}_{esc}$ and the velocity of the Earth through the halo, $\mathbf{v}_r$. We assume that the DM forms a nonrotating, isothermal, and spherically symmetric halo. In the galactic rest frame, the WIMP's are supposed to have a Maxwellian velocity distribution, with a velocity dispersion v_{rms}.

When the differential cross section is approximated by $d\sigma/dT = \sigma_p/T_{\max}$ (where σ_p is the elastic scattering cross section of the WIMP with a point-like nucleus and $T_{\max} = 2\mu^2v^2/M$ is the maximum recoil energy of the target nucleus) the differential energy spectrum becomes

$$\frac{dN}{dt\,dT} = N_D \frac{\rho_h}{m} \frac{\sigma_p M}{2\mu^2} I(T) \ ,$$

where $I(T)$ is the $v^{-1}f(\mathbf{v})$ weighted integral of those magnitudes which are velocity dependent, computed for the different approximations of v_{esc} and cross sections (see Ref. [14]). μ and M are, respectively, the WIMP-nucleus reduced and nucleus masses.

In the case of WIMP's with vector couplings to Z^0 bosons that scatter from nuclei by Z^0 exchange, the cross section is given by [15]

$$\sigma_p = \frac{G_F^2}{8\pi}\mu^2[Z(1 - 4\sin^2\theta_W) - N]^2 \ ,$$

where G_F is the Fermi coupling constant, Z and N are, respectively, the number of protons and neutrons in the target nucleus, and θ_W is the weak mixing angle.

The loss in coherence of the scattering process with the increase in linear momentum of the CDM relative to the target nuclei is accounted for, as usual, by correcting the cross section with a nuclear form factor $|F(q)|^2$ where $F(q)$, in the case of spin-independent interactions, is simply the Fourier transform of the nuclear density. In our calculation we have considered both Fermi and Gaussian nuclear distributions [14].

III. EXPERIMENTAL SETUP [8]

The COSME detector is a p-type coaxial hyperpure natural germanium crystal, of dimensions 22 mm (length)$\times$52.5 mm (diameter) corresponding to an active volume of 44 cm^3 and a mass of 234 g which has a long term resolution of 0.43 keV full width at half maximum (FWHM) at 10.37 keV and an energy threshold of 1.6 keV at 99% C.L. (stated at 2.33σ above the center of the Gaussian noise peak). The detector is of a dipstick type and was especially built for dark matter searches, i.e., with a low energy threshold and ultralow background materials. The cryostat, of 1.5 mm thick electroformed copper, has been made by Battelle Pacific Northwest Laboratory (PNL). The field effect transistor (FET) is shielded with 450 yr old (Spanish) lead. In the lower part of the cryostat cap, over the germanium crystal, there is a lead cylinder with a small aluminum and copper bar to produce x-rays for calibration when a suitable source is applied. A schematic view of the experimental setup is depicted in Fig. 1.

The detector is placed within a shielding of 10 cm of 2000 yr old (Roman) lead (inner layer) plus 20 cm of low activity lead (about 100 yr old). A 3 mm thick PVC box sealed with silicone closes the lead shielding to purge the radon gas by means of a 4 mm diameter Teflon conduction tube entering the box and allowing the boil-off nitrogen gas from the Dewar to circulate through the inner cavity. The PVC box is covered by 1 mm of cadmium and 20 cm of paraffin and borated polyethylene. In order to avoid the vibrations transmitted to the detector and cryostat through the floor and through the experimental assembly, as well as to prevent airborne vibrations, all the shielding and mounting is supported by 10 cm of vibrational and acoustic insulator sandwiched within two layers of 10 cm of wood mounted on a floor of concrete (20 cm). Care has been taken to eliminate electromagnetic and power line frequency interferences. In particular, we have paid special attention in shielding the cables from stray electromagnetic fields and in impedance matching to avoid signal distortion from reflections. The experimental setup is placed in the Underground Laboratory of the Zaragoza University, at the Canfranc tunnel (Spanish Pyrenees) at a depth of 675 m of water equivalent.

To improve the background and performances of the detector the remaining microphonic noises should be reduced as much as possible, and so we have developed an acquisition system [16] which filters a significant part of the microphonic noise which can be produced by environmental acoustic noise, bubbling and turbulences in the liquid nitrogen of the Dewar affecting the detector cryostat, vibrations in surrounding equipment, and other causes. Sources of electronic noise include fluctuations in the leakage current of the detector and thermal noise in the FET at the input of the preamplifier. In the very low energy region of the spectrum, above 1.5–2 keV, the noise is mainly caused by microphonics.
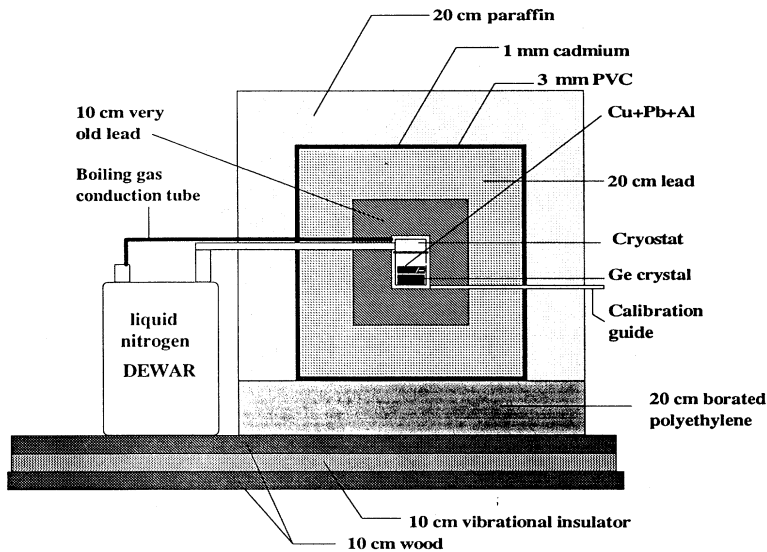
FIG. 1. Scheme of the COSME shielding and of the COSME detector itself.

To deal with the suppression of the microphonics and electronic noise several methods have been used in the past [17–19]. In this work we use a method of filtering the microphonic noise [16] based on the simultaneous use of two different shaping times in the processing of the signal. The method relies on the assumption [20] that normal (signal) and abnormal (noise) pulses have different rise times and distinctive general features, and so they are amplified differently for a chosen shaping time. Each arriving pulse is split and amplified along two paths with different shaping times. For normal pulses (generated by the detector itself) the ratio of the two amplified pulses is approximately a constant. For those external (abnormal) pulses generated by, say, microphonics, the ratio of the two outputs is not a constant and they can be rejected. On the other hand, as the microphonic pulses, or other spurious external pulses, come in bursts, events not distributed evenly in time are also excluded [7]. Recorded events arriving within a time interval of a second have been eliminated. Because of the low counting rates of the experiment, approximately 9 counts/h, no appreciable reduction of the counting time is produced. The combined use of both filtering procedures turns out to be an effective system of noise removal as is detailed in Ref. [16].

The readout electronics are based on standard NIM (Nuclear Instrument Module) modules plus an interface module, ALF, designed for this experiment. The output of the preamplifier is split to three separate linear amplifiers (Canberra 2020). The unipolar output signals of each one of the spectroscopy amplifiers are transferred to their respective analog-to-digital converters (ADC's) (Canberra 8075) into a range of 8192 channels. Their digital output lines are connected to a PC-Lab 720 II-A parallel digital I/O & Counter card, which has been installed on an expansion slot of an AT286 computer, through the interface module ALF mentioned above. Data from the converters are read by the acquisition program when one of the ADC's receives a "data ready" signal. The energies, arrival times, and a configuration word, built with the "data ready" signals of each event, are recorded. Be-

cause of the low counting rate (a few counts per hour) and fast readout, dead time caused by this process is negligible.

As far as the processing of the signal is concerned, in the first two paths, the gain is large (about 0.06 keV/channel). The only difference between the first and second lines is the shaping time in the main amplifiers, which was set to 3 and 4 μs, respectively (any other pair of suitable values can be used). That distinction allows us to separate true signal counts from noise, as stated before. The gain of the third line, however, is set on a much smaller value (0.35 keV/channel), to record events up to about 3 MeV, in order to identify radioactive nuclides contributing to the background.

The two methods of microphonics removal complement each other and the results are illustrated in Fig. 2 which displays the energy spectrum with and without filtering, showing an important reduction of the background in the low energy region from 1 to 10 keV.
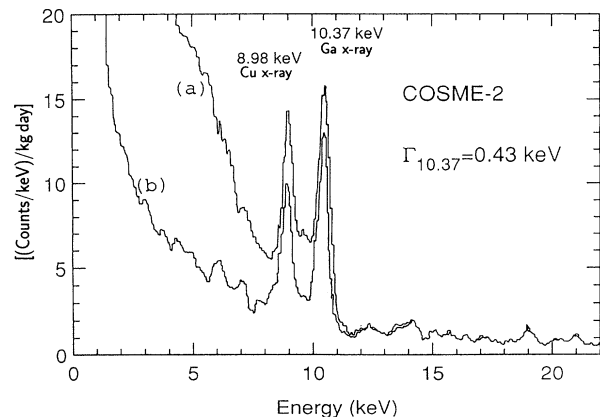

FIG. 2. COSME spectrum with (b) and without (a) filtering of the microphonics and electronic noise. The threshold energy is 1.6 keV, and the energy resolution at 10 keV is 0.43 keV.

IV. EXPERIMENTAL RESULTS

The filtered spectrum shown in Fig. 2 gives the experimental differential rate corresponding to $Mt = 130.7$ kg day of analyzed data. Some peaks which appear clearly in the spectra are the K-shell binding energies of Cu (8.98 keV) and Ga (10.367 keV), cosmogenically induced in the detector, both clearly resolved and not affected by the filtering procedures previously discussed.

The constraints on the cross sections and masses of CDM particle candidates imposed by the experimental data in Fig. 2 will be derived from both the filtered spectrum and successive considerations of various well-known residual spectra. The continuum due to the ^{68}Ga positron decay is negligible [14] in the low energy region relevant to the analysis. Tritium originating from spallation reactions accounts, at most, for 3% of the total number of counts (x-ray peaks excluded) of our background spectrum up to 18.6 keV and, very likely, could even be negligible [21]. There are also some other components of the spectrum which cannot be assigned to dark matter particles.

In general, if the predicted signal is larger than that observed, the particle under consideration may be ruled out to an extent that depends on the statistical method being used. In particular, to impose bounds on σ for a given mass m, we require that the number of predicted dark matter counts N_{th} in an energy bin (of about 2 keV for an energy resolution of 0.43 keV and a gain of 0.06 keV/channel) cannot be larger than the upper limit of the observed signal S (at a given confidence level) in the case of N_0 observed counts in a Poisson process. The Poisson-without-background case means that the raw experimental spectrum is supposed to constitute, entirely, the dark matter signal. The Poisson-with-background case means that the observed spectrum accounts for the dark matter signal plus successive (and cumulative) background contributions coming from various sources. Other statistical criteria may be and have been used in our analysis, with similar results [14]. We present in Fig. 3

the exclusion plots in the cross-section–mass plane (for $\rho_h = 0.3 \, \text{GeV cm}^{-3}$, $v_r = 230 \, \text{km s}^{-1}$, $v_{rms} = 300 \, \text{km s}^{-1}$, and $v_{esc} = 570 \, \text{km s}^{-1}$) derived from the spectrum of Fig. 2 corresponding, respectively, to the sum of successive background contributions to the spectrum, due to the x-ray peaks, to the radon contribution (estimated through an experimental measurement of its continuum spectrum) [14], and to a contribution of the continuum due to background sources and not to dark matter, because for a given mass no dark matter signal can appear above the corresponding T_{max} and therefore a linear extrapolation of the spectrum above T_{max} could account for the background at lower energies. Finally, the contribution of the few counts due to tritium β decay is included [21]. The region in parameter space contained within the curves in Fig. 3 is excluded for CDM candidates. In particular, the range of excluded masses for heavy Dirac neutrinos is shown in the intersection with the $\sigma_\nu(m)$ line, i.e., above 9.2 GeV and up to about 2.0 TeV (at 95% C.L.). The improvement in the exclusions when known backgrounds are considered is apparent in the figure. The degree to which this is a useful strategy depends on our knowledge of the sources of background and our ability to model their contributions to the spectrum. As can be seen from the figure, the low mass bounds are not sensitive to the cumulative background contributions considered. Similar results have been obtained in other experiments [5–7,10] excluding Dirac neutrinos of masses ranging from 9.2 GeV (this experiment) to 4.8 TeV (Ref. [10]).

Only one class of particle candidate has been supposed to constitute the galactic dark matter, and therefore the validity of the results is limited to the number density assumed for the DM candidate. As an alternative, the cross section can be fixed, and results can be plotted in the halo-density–mass parameter space. This approach is illustrated in Fig. 4 for the case of heavy Dirac neutrinos. The horizontal line labeled "halo density" corresponds to $\rho_h = 0.3 \, \text{GeV cm}^{-3}$ (the same parameter values as in Fig. 3 have been used to compute the rates).

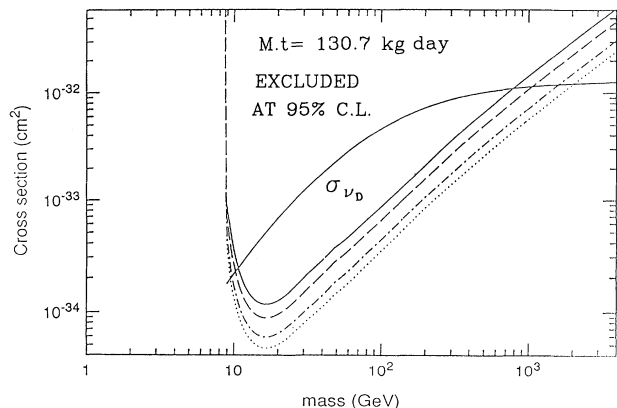The most important source of uncertainty in this type

FIG. 3. Exclusion plots for Dirac neutrinos at 95% C.L. Different background contributions have been cumulatively taken into account: peaks (solid line), ^{222}Rn (dashed line), Compton (dash-dotted line), and tritium (dotted line).
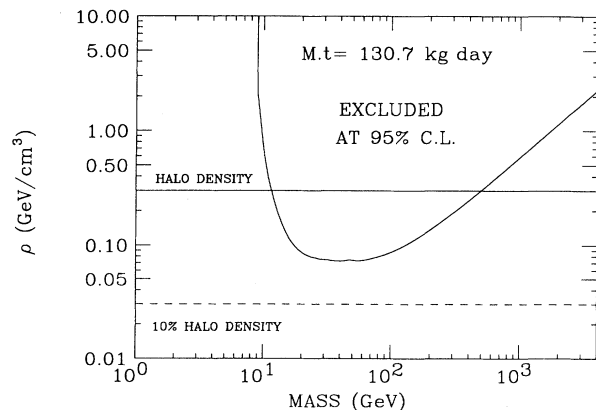

FIG. 4. Limits on the local abundance of heavy Dirac neutrinos obtained at 95% C.L. from the raw experimental spectrum.

of analysis is our lack of knowledge of the precise value of ρ_h, as well as the composition of the halo itself. In light of the new MDM approach [3], the bounds obtained for CDM particles with our germanium detector data should be drawn from a smaller value of the local number density of WIMP's. Figure 4 shows the CDM constraints remaining after a reduction of ρ down to 0.03 GeV cm^{-3}. That would be the case if the overall mass of the halo is smaller and/or when a detectable WIMP shares this mass with other candidates which are invisible to our detector. As can be seen, the constraints derived before for a standard, larger halo density disappear.

V. LOOKING FOR DISTINCTIVE SIGNALS OF DARK MATTER

As stressed above, the presence of a genuine feature of the DM in the data, not shared by the background, would be the only way to identify the DM. We will comment in the following on the results of a search for two such distinctive DM signals carried out with the COSME detector.

A. Diurnal modulation

The diurnal modulation [11] relies on the effects of elastic scattering of CDM particles with the Earth. The WIMP's scatter elastically off the Earth's constituent nuclei, giving rise to variations in flux and speed distribution of the WIMP's arriving at the detector. The scattering results in energy losses of the WIMP's and in redistribution of their exit points on the Earth's surface. This effect is more or less noticeable according to the cross section and mass of the WIMP.

The azimuthal symmetry of this effect around the direction of motion of the Earth through the halo, $\mathbf{v}$, defines a set of "isodetection rings" concentric around the axis defined by $\mathbf{v}$. At any given instant, all points on the Earth's surface belonging to the same isodetection ring experience an identical flux and velocity distribution of WIMP's. As the Earth rotates around its axis, the detector, placed at a given longitude and latitude, crosses a number of isodetection rings (see Fig. 5). For each
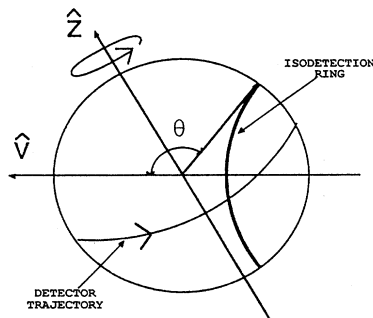
isodetection ring (specified by an angle $\theta \in [0°, 180°]$) the flux and velocity distribution of the WIMP's are different, and so is the DM signal. One then chooses two times t_1 and t_2 of the day (or equivalently the two groups of isodetection rings at $\Delta\theta_1$ and $\Delta\theta_2$ which the detector crosses at times t_1 and t_2) where the predicted Earth scattering effects of the WIMP's differ the most and compares the experimental data at these two times. Differences between the two sets of data (residual spectra) for each energy bin should be zero within expected statistical fluctuations in the absence of CDM elastic scattering in the Earth. If CDM particles do exist with masses and coupling constants that lead to even small diurnal modulations, the experimental residual spectrum will show a deviation from zero which varies with the energy bin.

In the case of our experiment, we have selected two bands of the COSME spectrum, $70° < \Delta\theta_1 < 83°$ and $12° < \Delta\theta_2 < 34°$, representing ranges of θ where the expected Earth scattering effects are maximally different for this detector's location. A standard hypothesis testing technique was used to compare the Monte Carlo calculated residuals with the experimental ones and to extract [14] the exclusion limit depicted in Fig. 6 for an exposure of $Mt = 84$ kg day. The location of COSME ($43°$ north latitude) together with the small statistics renders these limits less sensitive than those extracted from conventional methods. The sensitivity of the diurnal modulation method improves with the addition of new data or detector mass. This is a clear advantage over the signal-to-noise methods described above, where the addition of new data in the absence of an improvemet in the background yields no significant increase in the sensitivity of the search.

The motion of the rotating Earth through the galactic halo takes place in such a way that locations in the southern hemisphere are ideal to detect this daily fluctuation. This is due to the eclipsing effect of the dense iron-rich core of the Earth. Figure 6 also displays the predicted sensitivity of a detector with identical characteristics to COSME, situated at an optimal southern latitude. A dedicated search (COSME-SUR experiment) in the Sierra Grande mine, Rio Negro province (Argentina), by

FIG. 5. The geometry of the diurnal modulation method; shown are the velocity of the Earth through the galactic halo, $\hat{\mathbf{v}}$, the Earth's axis of rotation, $\hat{\mathbf{z}}$ and the isodetection rings on which the CDM velocity distribution and flux are uniform.
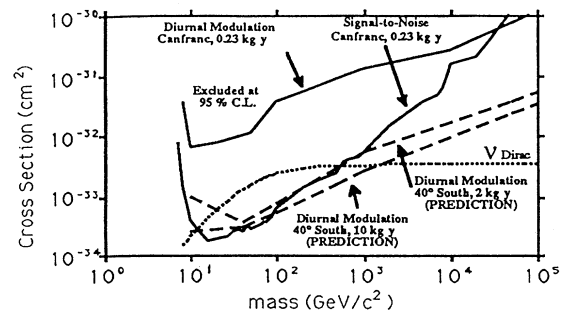
FIG. 6. Exclusion plots from the COSME detector using the standard method and from a search for diurnal modulations in the data. The two broken exclusion curves show the level of sensitivity obtainable with the diurnal modulation method at an optimal geographical location.

the TANDAR/CNEA and USC/PNL/Zaragoza groups has already started.

B. Annual modulation

The yearly modulation [12,13] takes advantage of the seasonal variation in the relative velocity v_r of the Earth and the galactic halo due to the Earth's rotation around the sun. The sun moves around the galaxy at a velocity of 232 ± 20 km s^{-1}, and the Earth moves around the Sun with an orbital speed of 30 km s^{-1} in an orbit whose axis makes an angle of $\delta = 30.7°$ with respect to the vector velocity of the Sun. The resulting net speed of the Earth with respect to the halo's reference frame oscillates with a period of one year, with maximum and minimum values in June and December, respectively, and so does the maximum amount of energy that can be deposited by the WIMP's in the detector, as well as the detection rates. For the annual modulation analysis, we shall use the parameter values of Ref. [13].

Since the velocity v_r changes as $v_r(t) = 232(\pm 20) + 15.3 \cos[\omega(t - t_0)]$, the expectd signal can be expressed in first order as a constant term plus a modulation component:

$$S(t) = S_0 + S_m \cos[\omega(t - t_0)] ,$$

where S are the detection rates derived from Sec. II.

Several approaches can be used to analyze the annual modulation. A naive estimate is to compute the average of the rates around the maximal and minimal expected values (June 2 and December 4) and compare the predicted difference with the observed one.

A more involved statistical analysis [13] of the effect is to study the modulation significance variable defined as $R = X/\sigma(X)$ where

$$X = \sum_{N \text{ years}} 2 \cos(\omega t_i)[S(t_i) + B(t_i)] .$$

$S(t_i)$ and $B(t_i)$ are Poisson random variables representing, respectively, signal and background collected data in a time bin of width τ (say 1 day) centered at time t_i. For a year-long experiment, R, which contains phase and amplitude information about the signal, can be approximated by $r = x/\sqrt{2d_{\text{ann}}}$, where x is the measurement of X for 1 yr and d_{ann} that of $D_{\text{ann}} = S + B$. If there is no modulation, r is Gaussian distributed around zero, with $\sigma = 1$. The confidence level to which a measurement r_0 of the modulation significance variable R can be said to be due to a real modulation of the signal is
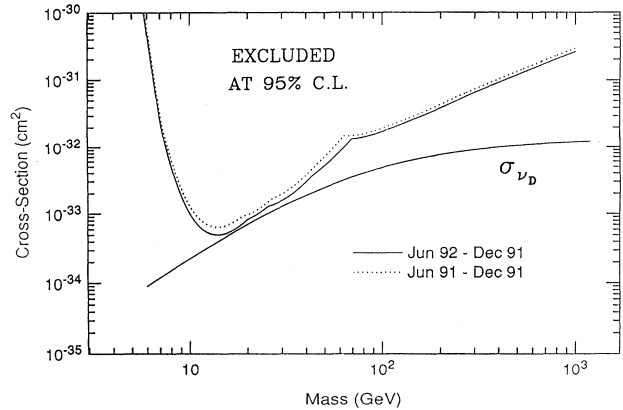

FIG. 7. Contour limits at 95% C.L. for Dirac neutrinos obtained from the difference of rates method in a search for annual modulation.

$$\text{C.L.} = \tfrac{1}{2} + \tfrac{1}{2}\text{erf}\left[\frac{r_0}{\sqrt{2}}\right] .$$

Notice that values of r_0 above 1.29 (90%) will be a fair indication of the existence of an annual modulation. In the case of not having collected data every day, one approximates r by $r = x/\sqrt{4\alpha d_{\text{ann}}}$ where $\alpha = 0.5114$ for the analyzed COSME data.

We have applied both approaches of annual modulation analysis to the COSME data registered over more than one year. No background has been removed and only paired days (opposite in the cosine period) have been selected.

By comparing the differences of rates, one gets results compatible with the absence of a modulation. Contour limits in the plane cross section vs mass can be obtained from the comparison of the experimental and theoretical residual spectra (Fig. 7). On the other hand, no presence of modulation is detected through the modulation significance method. We obtain, in fact, average values for the confidence levels $\langle \text{C.L.} \rangle = 0.55 \pm 0.31$ within those expected in the absence of modulation.

ACKNOWLEDGMENTS

[1] J. R. Primack, D. Seckel, and B. Sadoulet, Annu. Rev. Nucl. Part. Sci. **38**, 751 (1988).

[2] P. F. Smith and J. D. Lewin, Phys. Rep. **187**, 203 (1990).

[3] J. Ellis, in *TAUP 93*, Proceedings of the Third International Workshop on Theoretical and Phenomenological Aspects of Underground Physics, Gran Sasso, Italy, edited by C. Arpesella, E. Bellotti, and A. Bottino [Nucl. Phys. B (Proc. Suppl.) **35**, 5 (1994)]; J. A. Frieman, "Some Recent Developments in Cosmology: Dark Matter, Inflation and COBE," Report No. FERMILAB-

Conf 93/080-A, 1993 (unpublished); E. Gates and M. S. Turner, Phys. Rev. Lett. **72**, 2520 (1994).

[4] B. Sadoulet, in *TAUP '93* [3], p. 117; A. Milsztajn, *ibid.*, p. 137.

[5] S. P. Ahlen, F. T. Avignone, R. L. Brodzinski, A. K. Drukier, G. Gelmini, and D. N. Spergel, Phys. Lett. B **195**, 603 (1987).

[6] D. O. Caldwell, R. M. Eisberg, D. M. Drumm, M. S. Whiterell, B. Sadoulet, F. S. Goulding, and A. R. Smith, Phys. Rev. Lett. **61**, 510 (1988); D. O. Caldwell, B. Magnusson, M. S. Whiterell, A. Da Silva, B. Sadoulet, C. Cork, F. S. Goulding, D. A. Landis, N. W. Madden, R. H. Pehl, R. Smith, G. Gerbier, E. Lesquoy, J. Rich, M. Spiro, C. Tao, D. Yvon, and S. Zylberajch, *ibid.* **65**, 1305 (1990).

[7] D. Reusser, M. Treichel, F. Boehm, C. Broggini, P. Fisher, L. Fluri, K. Gabathuler, H. Henrikson, V. Jörgens, L. W. Mitchell, C. Nussbaum, and J. L. Vuilleumier, Phys. Lett. B **255**, 143 (1991).

[8] E. García, F. T. Avignone, R. L. Brodzinski, J. I. Collar, H. S. Miley, A. Morales, J. Morales, R. Núñez-Lagos, J. Puimedón, J. H. Reeves, C. Sáenz, and J. A. Villar in *TAUP '91*, Proceedings of the Second International Workshop on Theoretical and Phenomenological Aspects of Underground Physics, Toledo, Spain, edited by A. Morales, J. Morales, and J. Villar [Nucl. Phys. B (Proc. Suppl). **28A**, 286 (1992)].

[9] J. I. Collar, F. T. Avignone III, R. L. Brodzinski, E. García, H. S. Miley, A. Morales, J. Morales, R. Núñez-Lagos, J. Puimedón, J. H. Reeves, C. Sáenz, A. Salinas, M. L. Sarsa, and J. A. Villar, in *Neutrino'92*, Proceedings of the XVth International Conference on Neutrino Physics and Astrophysics, Granada, Spain, edited by A. Morales [Nucl Phys. B (Proc. Suppl.) **31**, 377 (1993)].

[10] M. Beck, in *TAUP '93* [3], p. 150.

[11] J. I. Collar and F. T. Avignone III, Phys. Rev. D **47**, 5238 (1993); Phys. Lett. B **275**, 181 (1992); J. I. Collar, F. T. Avignone III, R. L. Brodzinski, E. García, H. S. Miley, A. Morales, J. Morales, R. Núñez-Lagos, J. H. Reeves, C. Sáenz, and J. A. Villar, in *TAUP '91* [8], p. 297.

[12] A. K. Drukier, K. Freese, and D. N. Spergel, Phys. Rev. D **33**, 3495 (1986).

[13] K. Freese, J. Frieman, and A. Gould, Phys. Rev. D **37**, 3388 (1988).

[14] J. I. Collar, Ph.D. thesis, University of South Carolina, 1992; E. García, Ph.D. thesis, Universidad de Zaragoza, 1992.

[15] M. Goodman and E. Witten, Phys. Rev. D **31**, 3059 (1985).

[16] J. Morales, E. García, A. Ortiz de Solórzano, A. Morales, R. Núñez-Lagos, J. Puimedón, C. Sáenz, and J. A. Villar, Nucl. Instrum. Methods Phys. Res. Sect. A **321**, 410 (1992).

[17] F. S. Goulding, Nucl. Instrum. Methods **100**, 493 (1972); F. S. Goulding and D. A. Landis, IEEE Trans Nucl. Sci. **NS-29**, 1125 (1982).

[18] E. Gatti and P. F. Manfredi, Nucl. Instrum. Methods Phys. Res. Sect. A **226**, 142 (1984); Nuovo Cimento **9**, 3 (1986).

[19] N. N. Fedyakin *et al.*, Nucl. Instrum. Methods Phys. Res. Sect. A **292**, 450 (1990).

[20] F. S. Goulding, presented at the 1st Workshop on Low Background Experiments, Berkeley, 1989 (unpublished).

[21] F. T. Avignone, R. L. Brodzinski, J. I. Collar, H. S. Miley, E. García, A. Morales, J. Morales, R. Núñez-Lagos, J. H. Reeves, C. Sáenz, and J. A. Villar, in *TAUP '91* [11], p. 280.
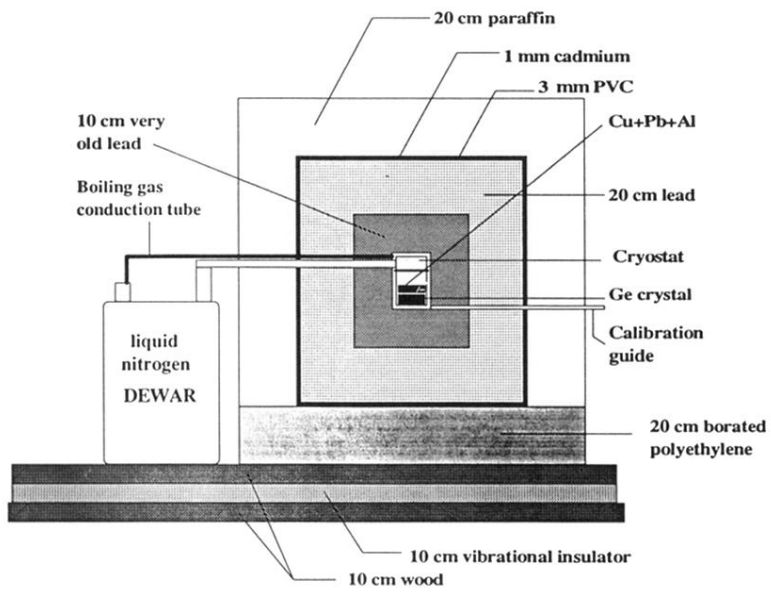
FIG. 1. Scheme of the COSME shielding and of the COSME detector itself.